



Aluminum diffusion and Al-vacancy association in periclase

James A. Van Orman*, Chen Li¹, Katherine L. Crispin

Department of Geological Sciences, Case Western Reserve University, 10900 Euclid Avenue, Cleveland, OH 44106, USA

ARTICLE INFO

Article history:

Received 14 September 2007

Received in revised form 20 February 2008

Accepted 20 March 2008

Keywords:

MgO

Point defects

Lower mantle

Core–mantle boundary

ABSTRACT

Trivalent cations in periclase are attracted to cation vacancies and these defects tend to associate on adjacent sites to form mobile pairs. A theory has been developed to describe the concentration-dependent diffusion of Al in the presence of Al-vacancy pairs, and has been applied to experiments conducted at 1577–2273 K and 1 atm to 25 GPa. In all but one experiment, the Gibbs free energy of binding, inferred from the diffusion profiles, is between –44 and –60 kJ/mol, with an average value of –50 kJ/mol. The absolute value of the entropy of binding is constrained to be less than $50 \text{ J mol}^{-1} \text{ K}^{-1}$, and the volume of binding is constrained to be between –1.8 and $0 \text{ cm}^3/\text{mol}$. The diffusion coefficient of the Al-vacancy pair can be described by the equation $D_2 = D_{2,0} \exp(-(E + PV)/RT)$, with $E = 213 \pm 32 \text{ kJ/mol}$, $V = 3.22 \pm 0.25 \text{ cm}^3/\text{mol}$, and $\log_{10} D_{2,0} = -6.17 \pm 0.99$ (in m^2/s ; all uncertainties 2σ). Calculations are presented for the diffusion of Al and Mg as functions of Al concentration, temperature and pressure.

© 2008 Elsevier B.V. All rights reserved.

1. Introduction

Periclase is thought to be the second most abundant mineral in Earth's lower mantle, comprising ~15–20% of the total mass (e.g., Bina, 1998). Cation diffusion in periclase is considerably more rapid than in the more abundant magnesium silicate perovskite (Yamazaki et al., 2000; Yamazaki and Irifune, 2003; Van Orman et al., 2003; Holzapfel et al., 2003, 2005; Mackwell et al., 2005), and periclase thus may enhance bulk diffusive transport in the lower mantle, especially in regions where it may be present in higher abundance. The core–mantle boundary may be one such region, as recent diamond anvil cell experiments show that FeO and SiO₂ have substantial solubility in molten iron at very high pressures, while MgO remains insoluble (Takafuji et al., 2005). It is thus plausible to speculate that dissolution of silicates has left a periclase-enriched layer at the base of the mantle, which would play an important role in regulating chemical exchange between the core and mantle.

Trivalent cations, including Al³⁺, Cr³⁺ and Fe³⁺, are significantly soluble in periclase (e.g., Wood, 2000; Watson and Price, 2002; Mackwell et al., 2005) and, if insufficient monovalent cations are available to maintain charge balance, their substitution on cation sites is coupled with the creation of cation vacancies. Because the formation energy of Schottky defects in periclase is very high

(Ita and Cohen, 1997), these extrinsic cation vacancies, present to balance the charge of trivalent cation impurities, are far more abundant than intrinsic Schottky vacancies even in very pure synthetic periclase samples, and thus control the diffusivity of cations that migrate by a vacancy mechanism (Sempolinski and Kingery, 1980). Periclase produced experimentally in peridotite bulk compositions at lower mantle pressures (Wood, 2000), and natural periclase found in diamond inclusions (Stachel et al., 2000) contain quite high concentrations of trivalent solutes, on the order of 1 wt% or more. Sodium also has relatively high abundance in these periclase crystals, but the cation fraction of Al³⁺ + Cr³⁺ + Fe³⁺ typically exceeds that of Na by ~3000–5000 ppm (if the reasonable assumption is made that ~3% of the iron present, on a cation basis, is ferric, as has been measured in iron-buffered experimental samples by Stretton et al., 2001). Trivalent cations are thus likely to have a strong influence on cation diffusion rates in periclase in Earth's lower mantle.

In the simplest case, the diffusion rate of a cation is proportional to the total cation–vacancy concentration. However, the situation in periclase is complicated by the Coulombic attraction between trivalent cations and cation vacancies, which have net charges of +1 and –2, respectively. This attraction may lead to the formation of tightly bound pairs (e.g., Gourdin and Kingery, 1979a,b; Sempolinski and Kingery, 1980; Carroll et al., 1988; Hirsch and Shankland, 1991), as illustrated schematically in Fig. 1. The formation of bound pairs has two important effects on diffusion. On one hand, association with a relatively immobile trivalent cation diminishes the mobility of the vacancy. This reduces both the ionic conductivity (which is controlled by cation–vacancy motion in periclase; Sempolinski

* Corresponding author.

E-mail address: james.vanorman@case.edu (J.A. Van Orman).

¹ Present address: Department of Geosciences, University of Arizona, Gould-Simpson Building #77, 1040 E 4th Street, Tucson, AZ 85721, United States.

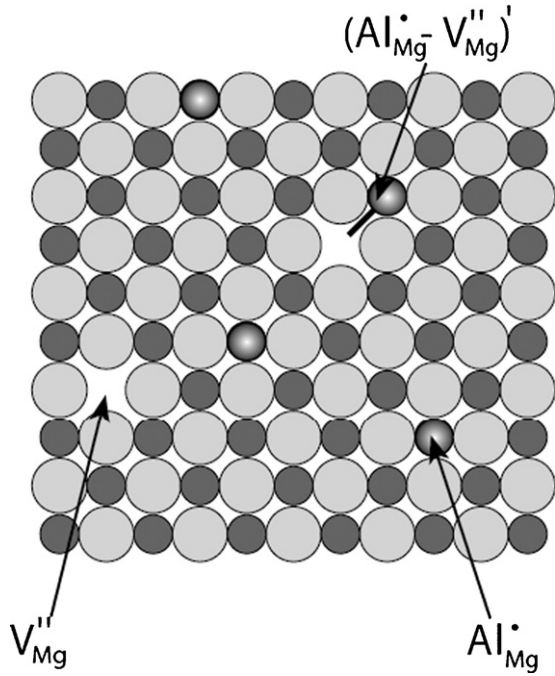


Fig. 1. Schematic 2D representation of periclase containing Al^{3+} solutes, showing isolated Al_{Mg}^+ (Al^{3+} atoms on cation sites) and V_{Mg}'' (vacant cation sites), and a defect pair consisting of an Al atom and vacancy on nearest-neighbor cation sites. Oxygen atoms are light grey, Mg atoms dark grey, and Al atoms have zoned shading.

and Kingery, 1980) and the diffusivity of unassociated cations that diffuse by a vacancy mechanism. On the other hand, association with a highly mobile vacancy significantly enhances the mobility of the trivalent cation (e.g., Van Orman et al., 2003). The enhanced mobility is due to the steady availability of a vacancy on an adjacent cation site, which increases the probability of an impurity-vacancy site exchange. Association with vacancies is thought to be responsible for the anomalously fast diffusion of divalent cations in alkali halides (e.g., Lidiard, 1955; Keneshea and Fredericks, 1963), and may also explain the rapid diffusion of trivalent REE relative to divalent cations in fluorite (Cherniak et al., 2001).

Van Orman et al. (2003) made a cursory investigation of Al diffusion in periclase at high pressure as part of a study of magnesium and oxygen self-diffusion in MgO. Here we revisit Al diffusion and Al-vacancy association in more detail, adding new experimental data at 1 atm to 15 GPa and 1577–1873 K, and presenting a new method for extracting the binding energy and diffusion coefficient of a trivalent cation-vacancy pair from an experimental diffusion profile. The data are used to calculate diffusion coefficients for Al and Mg in periclase as functions of temperature, pressure and Al concentration.

2. Theory

An Al^{3+} ion substituted on the Mg^{2+} site in MgO has a net charge of +1, which must be balanced by a negatively charged species to maintain electrical neutrality. The dominant negatively charged species in MgO is a cation-vacancy, which has a net charge of -2. Assuming that substitutional Al^{3+} ions and cation vacancies are the only aliovalent species in MgO, the electrical neutrality condition is expressed (in Kröger–Vink notation; e.g., Kröger, 1974) as:

$$[\text{Al}_{\text{tot}}] = [\text{Al}_{\text{Mg}}^+] = 2[V_{\text{Mg}}''] \quad (1)$$

In this expression, no assumptions are made about whether the Al ions and vacancies are associated with each other; the concen-

trations refer to the total fraction of cation sites that are occupied by Al, or are vacant, respectively.

Ferric iron has been found to occupy interstitial sites in periclase in minor but significant proportions (e.g., Jacobsen et al., 2002). This configuration appears to be stabilized by a cluster of surrounding cation vacancies (Gourdin and Kingery, 1979a,b). Al^{3+} might be expected to adopt a similar interstitial configuration due to its small size. However, these interstitial-vacancy clusters are thought to be significant only at low temperatures, less than ~ 1000 K (Carroll et al., 1988), and are not likely to be relevant at the higher temperatures considered here.

As noted in the introduction, Al^{3+} and cation vacancies are attracted electrostatically and tend to form bound complexes. A number of complexes may form, but those with three members or more (e.g., consisting of two trivalent cations and a single vacancy) generally are significant only at high impurity concentrations and/or low temperatures (Carroll et al., 1988; Hirsch and Shankland, 1991). At the moderate Al concentrations (< 5000 ppm) and high temperatures (> 1577 K) considered here, vacancies are expected to exist in significant proportion only in isolation, or as a two-member complex, bound to a single Al^{3+} ion. For simplicity we consider only defect pairs in which the Al^{3+} ion and vacancy exist on nearest-neighbor cation sites, not on second-nearest-neighbor or more distant sites.

Equilibrium between Al^{3+} , distant cation vacancies, and bound Al-vacancy pairs is described by the following equations:



where $(V_{\text{Mg}}\text{Al}_{\text{Mg}})'$ denotes the bound pair. The ideal mass action law for this reaction, assuming ideal solution of all species, can be written as follows (Lidiard, 1955):

$$K_2 = \frac{[(V_{\text{Mg}}\text{Al}_{\text{Mg}})']}{[V_{\text{Mg}}''][\text{Al}_{\text{Mg}}^+]} = Z_2 \exp\left(\frac{-G_2}{RT}\right) \quad (3)$$

where the brackets denote concentrations (molar fractions); G_2 is the free energy of association, or binding energy, of the pair; and Z_2 is the number of distinguishable orientations of the pair, in this case 12.

Following Lidiard (1955) and Perkins and Rapp (1973), it is convenient to rewrite Eq. (3) in terms of the fraction of Al^{3+} ions that exist in bound pairs (p) and the fraction of cation sites occupied by Al^{3+} (x_{Al}):

$$\left\{ \frac{p}{x_{\text{Al}}(1/2 - p)(1 - p)} = 12 \exp\left(\frac{-G_2}{RT}\right) \right\} \quad (4)$$

This can be rearranged to give an equation for p :

$$p = \frac{3}{4} + \frac{1}{2A} - \left(\frac{1}{16} + \frac{3}{4A} + \frac{1}{4A^2} \right)^{1/2} \quad (5)$$

where $A = 12x_{\text{Al}} \exp(-G_2/RT)$.

The concentration-dependent diffusion coefficient of aluminum in the presence of Al-vacancy pairs is governed by the diffusivity of the pair and the derivative of the pair concentration with respect to the total aluminum concentration (Lidiard, 1955; Perkins and Rapp (1973):

$$D_{\text{Al}} = D_2 \frac{d(px_{\text{Al}})}{d(x_{\text{Al}})} \quad (6)$$

where D_{Al} is the diffusion coefficient of Al at a given Al concentration, and D_2 is the diffusion coefficient of the Al-vacancy pair. Combining Eqs. (5) and (6) gives an expression for the diffusion coefficient of Al as a function of its total concentration and the free

energy of binding between Al^{3+} and cation vacancies:

$$D_{\text{Al}} = D_2 \left\{ \frac{3}{4} - \left(\frac{x_{\text{Al}}^2}{16} + \frac{x_{\text{Al}}}{16 \exp(-G_2/RT)} + \frac{1}{576 \exp(-2G_2/RT)} \right)^{-1/2} \right. \\ \left. \times \left(\frac{x_{\text{Al}}}{16} + \frac{1}{32 \exp(-G_2/RT)} \right) \right\} \quad (7)$$

This expression holds for all Al^{3+} concentrations, provided that Al-vacancy pairs on nearest-neighbor sites are the only complexes present.

Eq. (7) can be applied to experimental Al diffusion profiles provided that a local equilibrium is established between associated and unassociated Al atoms and vacancies along the profile. A simple calculation shows that local equilibrium is likely to be achieved. To form a pair requires that a vacancy diffuse into the vicinity of an Al atom. Even at a very low Al concentration (50 ppm) the average separation between Al atoms and vacancies is less than 10 nm, and the vacancy diffusion coefficient is quite high, $1.9 \times 10^{-12} \text{ m}^2/\text{s}$ even at 1573 K, the lowest temperature considered here (Sempolinski and Kingery, 1980). Thus, the average time required for a vacancy to diffuse into the immediate neighborhood of an Al atom is less than 10^{-4} s. Even if several encounters between a vacancy and Al atom are necessary to form a bound pair (only one encounter is required if the binding energy is high), local equilibrium will be established rapidly relative to the timescale of the diffusion experiment.

Fig. 2 shows how the proportion of Al-vacancy pairs and the Al diffusion coefficient vary with Al concentration, for three different values of the binding energy between Al^{3+} ions and cation vacancies. Note that at high Al concentrations and relatively large binding energies, the proportion of bound pairs asymptotically approaches 1/2 (i.e., essentially all cation vacancies are bound to Al atoms), and the Al diffusion coefficient approaches $D_2/2$.

3. Experiments

Experimental diffusion couples consisted of a single crystal of MgO surrounded by fine-grained MgAl_2O_4 spinel powder. The spinel powder was fabricated by glycine-nitrate sol-gel combustion synthesis (e.g., Chick et al., 1990), followed by a 24 h anneal in air at 900 °C. A 5 mol% excess of MgO was added to the sol-gel solution to ensure that the spinel was saturated with periclase. After annealing, the spinel powder was rinsed ultrasonically in a 1 M HNO_3 solution to dissolve any remaining MgO, and then rinsed again in purified water. The powder was analyzed with a Scintag X-1 powder X-ray diffractometer, and showed only sharp spinel peaks. The grain size of the spinel powder was not measured, but is believed to have been less than $\sim 10 \mu\text{m}$.

The MgO crystals used in the experiments were purchased from SPI and had a nominal impurity content, reported by the supplier, of 40 ppm Ca, 15 ppm Al, 50 ppm Fe, 10 ppm Cr and 5 ppm B. No attempt was made to measure the composition of the crystals to check whether the reported impurity contents were correct, but the nominal values are so low compared to the Al concentrations that were measured within the diffusion profiles that they are not expected to have had a significant influence on Al diffusion. No cations other than Mg and Al were detected by electron microprobe along any of the measured diffusion profiles. The $10 \text{ mm} \times 10 \text{ mm} \times 0.5 \text{ mm}$ MgO crystals were mirror polished on two sides, cleaved into pieces approximately 1 mm on a side, and heated in air at 1500 °C for several days to anneal surface damage caused by polishing.

In experiments at atmospheric pressure, an MgO crystal was packed in spinel powder within a Pt crucible and suspended in a Deltech vertical tube furnace that had been pre-heated to the run

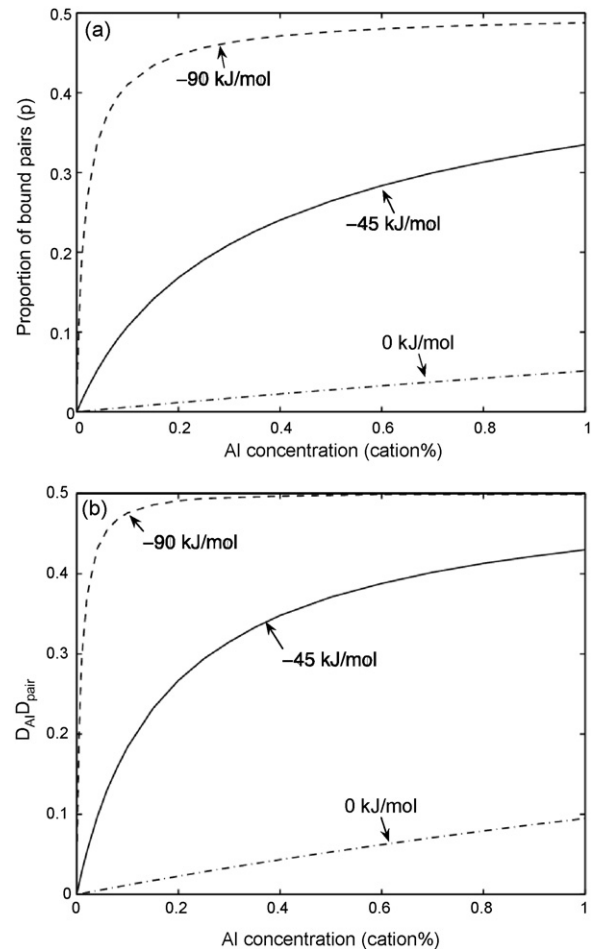


Fig. 2. (a) Proportion of Al atoms bound to a cation-vacancy, and (b) Al diffusion coefficient, normalized to the Al-vacancy pair diffusion coefficient, for periclase containing up to 1% dissolved Al (as cation fraction). Curves show solutions to Eqs. (5) and (7) for three different values of the free energy of binding between an Al solute and a cation-vacancy.

temperature. The temperature was measured continuously using a Type B Pt-Rh thermocouple, and fluctuated within less than 2 °C over the course of each experiment. Following the isothermal anneal, the sample was removed from the furnace and allowed to cool in air. The time to heat and cool each sample was less than a minute, very small compared to the isothermal anneal times, which ranged from 0.73 to 27.47 h. Thus no attempt was made to account for diffusion during heating and cooling of the experiment. The MgO crystals could be removed from the spinel powder after the experiment, usually with a small amount of powder adhering to the surface. There was no evidence for any chemical reaction between the spinel and MgO during any of the experiments. Where the polished surface of the MgO crystal was visible it maintained a mirror polish, and where the interface between MgO and spinel was visible in backscattered electron images (mainly in the high-pressure experiments described below) it was always observed to be a sharp boundary with no evidence for secondary phases.

High-pressure experiments were performed with a 1500-ton multi-anvil apparatus at the Geophysical Laboratory, using an 8/3 octahedral assembly with a cylindrical Re furnace and a W5%Re/W26%Re thermocouple placed near the diffusion couple. The diffusion couple was centered in the hotspot of the assembly and was bounded on top and bottom by alumina rods. Samples were heated at 100 K/min to the run temperature and quenched

by shutting off the power. As with the 1 atm experiments, heating and cooling times were insignificant compared to duration of the isothermal diffusion anneal. The difference in temperature between the thermocouple junction and diffusion interface was judged to be less than 20 K, based on the measurements of the temperature profile in this assembly using spinel growth kinetics (van Westrenen et al., 2003). The relative uncertainty in pressure is believed to be ~ 0.5 GPa (Bertka and Fei, 1997).

Following the diffusion anneal, the MgO crystal was mounted in epoxy and ground down at least 300 μm perpendicular to the diffusion interface. Samples were then polished with diamond suspensions to 0.25 μm and coated with a thin layer of carbon for electron microprobe analysis. Concentration profiles were measured with the JEOL 8900 electron microprobe at the Geophysical Laboratory, using a focused beam and wavelength dispersive spectrometry. The accelerating voltage was 15 kV and the probe current was 30 nA. Pure MgO and enstatite glass doped with 5 wt% Al_2O_3 were used as standards for Mg and Al, respectively. Linear scans were made perpendicular to polished surfaces that had been in contact with the spinel powder during the diffusion anneal. The distance between adjacent analyses was 2.5–10 μm , sufficient to avoid overlap between spots. Following the experiments the periclase crystals were found to be free of inclusions or other visible imperfections, other than some cracks in the crystals annealed at high pressure, which were avoided during the analysis. None of the Al diffusion profiles extended to the center of the crystal, so the diffusion geometry could in each case be treated as one-dimensional and semi-infinite. No attempt was made to measure diffusion profiles in the spinel. In the experiments at atmospheric pressure, little of the spinel powder adhered to the periclase crystal following the experiment, and it often could not be observed at all in the sections polished for microprobe analyses. A few scattered analyses of the spinel were made on the high-pressure samples, and these were nearly stoichiometric, with a small excess of MgO.

4. Diffusion coefficient and binding energy determination

As discussed above, diffusion of Al in MgO is strongly dependent on Al concentration, due both to the creation of cation vacancies to maintain electroneutrality and to the Coulombic attraction of these vacancies to positively charged Al cations. The differential equation for one-dimensional diffusion, when the diffusion coefficient is a function of concentration, is (e.g., Crank, 1975):

$$\frac{\partial C}{\partial t} = \frac{\partial}{\partial x} \left(D \frac{\partial C}{\partial x} \right) \quad (8)$$

where C represents the concentration, t the time, and x the distance. There is no general closed-form solution to this equation, and aside from a few special cases $D(C)$ has to be determined numerically. As noted above, these experiments could be considered to have an effectively semi-infinite geometry, and the spinel provided an effectively infinite reservoir of Al. Experiments annealed for different times extending over an order of magnitude at the same conditions had similar Al concentrations near the surface; there was no decrease in the interface concentration with time. There is nearly always some motion of the interface between two condensed phases when there is chemical transfer between them, unless the molar volumes of the species transferred are equivalent (e.g., Balluffi, 1960); however, interface motion was considered negligible in this case, since the Al concentration in the periclase was quite low and the diffusion profiles quite long. For diffusion in one-dimension, with semi-infinite geometry, constant surface concentration and an immobile boundary, and initial conditions $C = C_0$ at $x = 0$, and $C = 0$ for $x > 0$, Eq. (8) can be transformed into

an ordinary differential equation with the following solution (e.g., Shewmon, 1989, p. 36):

$$D(C) = \frac{-1}{2t} \left(\frac{dx}{dC} \right)_C \int_0^C x \, dc \quad (9)$$

where C is the concentration at a particular position along the diffusion profile. This equation is known as the Boltzmann–Matano equation and has been used widely over several decades to determine $D(C)$ directly from experimental diffusion profiles, but its application can be problematic. The slope at a particular position along the diffusion profile must be determined by fitting a curve to the data. In general, it is not known *a priori* which functional form is appropriate to model the data, and the fit of an arbitrary curve can introduce systematic errors in the determination of $D(C)$, as discussed, for example, by Holzapfel et al. (2003).

Here it was possible to take a somewhat different approach to determine diffusion coefficients, since the simple point defect model outlined in Section 3 gives the theoretical dependence of D_{Al} on Al concentration. For given values of D_2 (the Al-vacancy pair diffusivity) and G_2 (the Gibbs free energy of binding), the diffusivity of Al as a function of Al concentration was calculated according to Eq. (7). The Al diffusion profile for this set of parameters and the appropriate anneal time was then calculated numerically according to Eq. (9) using an iterative technique. An initial guess was made of the value of the integral from 0 to C_0 ; this was used to calculate the concentration profile stepwise from C_0 to 0, and from this profile a new value of the full integral was calculated. The process was repeated until the value of the full integral converged. Convergence was rapid for most reasonable initial guesses; typically the initial guess was in the neighborhood of $0.6C_0 \sqrt{D(C_0)t}$.

For each experiment a family of diffusion profiles was computed for different combinations of D_2 (the diffusivity of the Al-vacancy pair) and G_2 (the binding energy of the pair), and each was compared to the experimental diffusion profile. Best-fit values of the pair diffusivity and binding energy were determined for each experimental diffusion profile by minimizing χ^2 , and their associated uncertainties were estimated from a contour plot of χ^2 versus D_2 and G_2 (Fig. 3). The contours are elliptical because D_2 and G_2 are correlated in the fitting procedure; the correlation arises because an increase in either value raises the Al diffusion coefficient at a given concentration. Because D_2 and G_2 were positively correlated, the uncertainty in determining each parameter was sometimes fairly large, but in most cases the binding energy for different profiles on the same sample was reproducible within less than 30% (2σ) and the pair diffusion coefficient within less than 75% (2σ). For most profiles, the value of reduced χ^2 for the best-fitting profile was between 0.5 and 2, which indicates good agreement between the data and model.

5. Results

Values of the diffusion coefficient and binding energy of the Al-vacancy pair, obtained from the numerical fitting procedure described above, are listed in Table 1. The table includes data from two experiments reported in Van Orman et al. (2003), which were re-analyzed here with a denser spacing of microprobe spots.

Experiments performed at similar conditions for different times yielded consistent results. Fig. 4 shows diffusion profiles from four experiments performed at atmospheric pressure and 1670–1674 K, with run durations between 2.54 and 19.38 h. When the geometry is infinite or semi-infinite, as in these experiments, a profile of concentration versus x/\sqrt{t} should not vary with time, regardless of how the diffusion coefficient varies with concentration. When plotted in this way all of these profiles fall within a narrow band, which

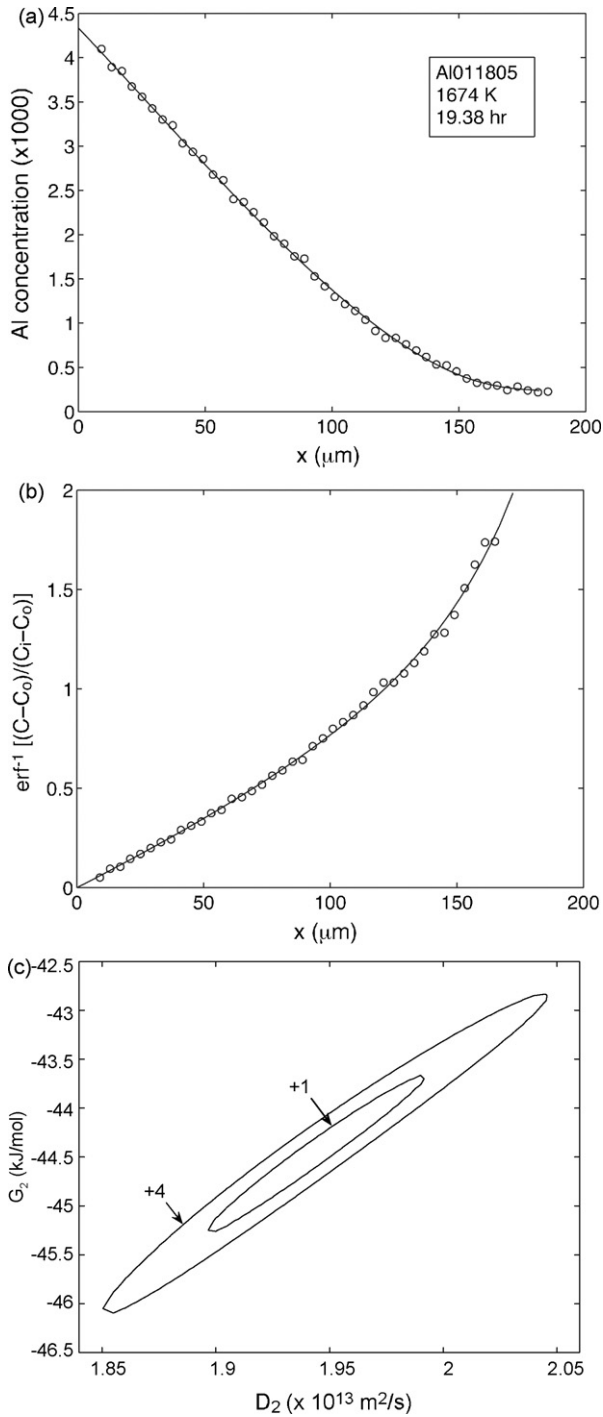


Fig. 3. A typical Al diffusion profile from (a) 1 atm experiment, with concentration expressed as cation fraction. The profile is shown in (b) as the inverse error function of the normalized concentration. If the diffusion coefficient were constant the profile would be linear on this inverse error function plot; its concave upward curvature indicates that the diffusion coefficient decreases with increasing concentration. The solid curves show a numerical solution to the diffusion equation with the Al diffusion coefficient given by Eq. (7). A family of such curves was calculated for different combinations of the Al-vacancy pair diffusion coefficient (D_2) and binding energy (G_2), and the best fit was determined by χ^2 minimization. A contour plot of χ^2 versus D_2 and G_2 is shown in (c), with the contours representing values of $\chi^2 + 1$ and $\chi^2 + 4$. The horizontal and vertical limit of the $\chi^2 + 4$ contour give estimates of the uncertainty in D_2 and G_2 , respectively, for each profile. However, the uncertainties listed in Table 1 were determined from the reproducibility in the values from several different diffusion profiles measured on the same experimental sample.

Table 1
Summary of experimental conditions and results

Expt #	T (K)	P (Pa)	Anneal time (h)	D_2 (10^{-13} m ² /s)	G_2 (kJ/mol)
pcMgO2*	2273	1.5e10	9.50	8.45(0.98)	-50.0(3.4)
pcMgO3*	2273	2.5e10	8.87	1.50(0.13)	-95.8(17.0)
M858	1873	1.5e10	4.10	1.64(0.60)	-53.1(16.0)
AlO20705-1	1767	1.01e5	1.05	3.11(1.8)	-57.6(17.8)
Al120304	1768	1.01e5	0.73	3.23(0.64)	-59.7(3.0)
AlO11805	1674	1.01e5	19.38	2.02(0.58)	-43.8(8.2)
AlO20605	1670	1.01e5	8.72	1.46(0.37)	-51.5(4.6)
Al120704	1673	1.01e5	5.63	1.81(1.19)	-53.7(13.8)
AlO20705†	1670	1.01e5	2.53	N/A	N/A
Al120404	1578	1.01e5	27.47	0.678(0.347)	-49.4(12.8)
AlO12505	1577	1.01e5	24.28	0.552(0.107)	-59.0(6.6)

Uncertainties (given in parentheses) are standard deviations (2σ) determined from three to four replicate measurements of the concentration profile at different locations on each charge.

* Preliminary results on Al diffusion from these two experiments were reported by Van Orman et al. (2003). The concentration profiles were re-analyzed and fitted according to the numerical model described in the text.

† Profiles in this experiment could not be fit to simultaneously determine the pair binding energy and diffusivity; the two parameters were highly correlated and the range of values fitted to 67% confidence was very large. If the binding energy is assumed to be -50.1 kJ/mol (the average value determined from other experiments at atmospheric pressure) the pair diffusion coefficient is determined to be $2.36(1.36) \times 10^{-13}$ m²/s, consistent with the other experiments at similar temperatures.

indicates that diffusion is the primary transport process and gives a measure of the experimental reproducibility. The best-fit values of the Al-vacancy pair diffusion coefficient and binding energy for these experiments are consistent within mutual uncertainty, and show no significant dependence on time (Fig. 4c).

With one exception—the experiment at highest pressure, 25 GPa and 2273 K—the best-fit value of the Gibbs free energy of association for each experiment falls within the range -44 to -59 kJ/mol, with an average value of -50.1 kJ/mol. These values are somewhat smaller than theoretical binding energies obtained at 0 K from shell model calculations. Gourdin and Kingery (1979a,b) calculated a value of -65.5 kJ/mol, and Carroll et al. (1988) obtained values of -63 and -69 kJ/mol using two different interionic potentials. Extrapolating these values to the temperatures investigated here brings them into closer agreement with our experimental results. Assuming that the temperature dependence was associated mainly with lattice expansion, Carroll et al. (1988) calculated that the binding energy would be 23% less at 1500 K. Similarly, an experimental study by Gourdin and Kingery (1979a,b) of the association between Fe³⁺ and cation vacancies yielded a value for the binding energy 19% lower at 1400 °C than the shell model calculation of Gourdin and Kingery (1979a,b).

The lack of a resolvable temperature dependence of the binding energy implies that the entropy change of the Al³⁺-vacancy association reaction is relatively small. An upper limit on the entropy of the association reaction can be obtained by considering the 1 atm experiments, for which the free energy of the reaction could be resolved to within ~5–10 kJ/mol. This implies that the absolute value of the binding entropy must be less than ~25–50 J mol⁻¹ K⁻¹, which is consistent with the value of 13 J mol⁻¹ K⁻¹ estimated for the Fe³⁺-vacancy association reaction (Hirsch and Shankland, 1991).

The 25 GPa experiment has a significantly higher binding energy (-96 kJ/mol) than the other experiments, which might indicate that Al cations and vacancies become more tightly bound at very high pressures. However, two experiments at 15 GPa yielded binding energies of -50 and -53 kJ/mol, near the middle of the range for the 1 atm experiments. Considering only the 1 atm experiments and the 25 GPa experiment gives $V \sim -1.8$ cm³/mol for the Al³⁺-vacancy association reaction, but if only the 1 atm and 15 GPa experiments

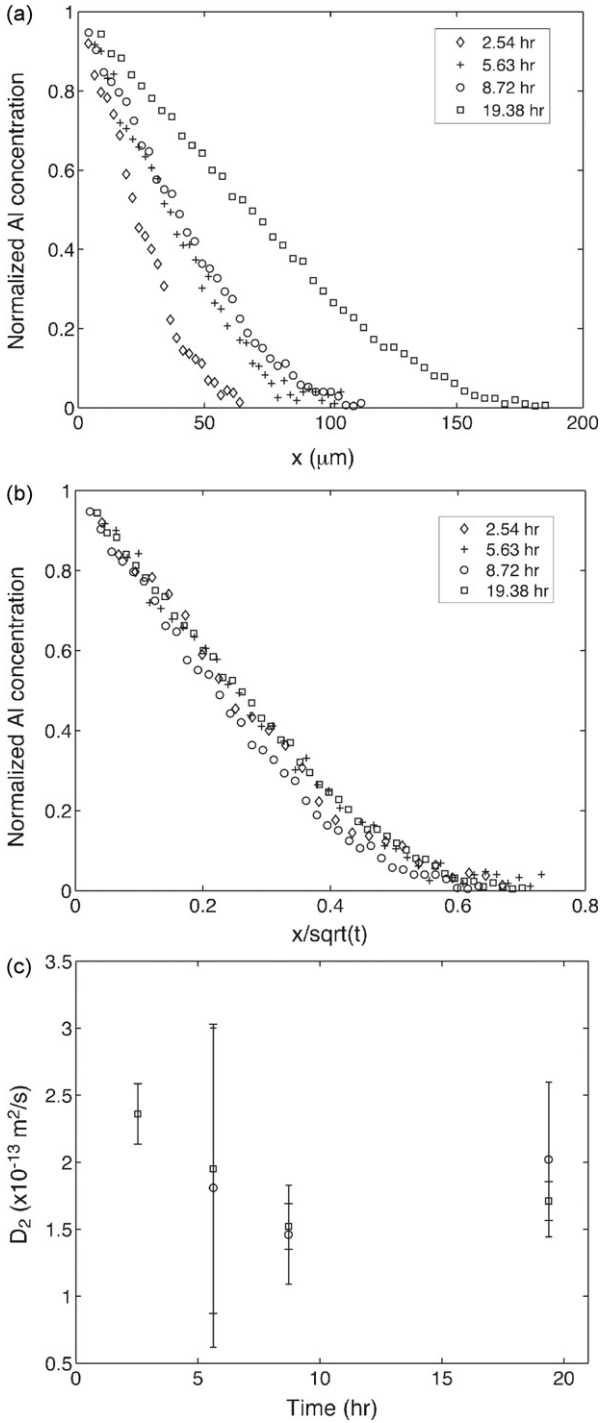


Fig. 4. Results of a time series conducted at 1672 ± 2 K. (a) shows concentration profiles from four different experiments, and (b) shows the same profiles, but with the distance from the interface (in μm) scaled by the square root of the run duration (in seconds). On this plot all four profiles overlap within a narrow band, consistent with transport by volume diffusion. In (c) the Al-vacancy pair diffusion is plotted against time. Circles show best-fit diffusion coefficients from Table 1; squares show the best-fit values when the binding energy is set at -50.1 kJ/mol.

are considered, $V \sim 0$. A more detailed high-pressure study would be necessary to place tighter constraints on the pressure dependence of Al^{3+} -vacancy association, but in any case it is clear that the volume change is quite small. This is qualitatively consistent with theoretical calculations, in which the relaxations of oxygen

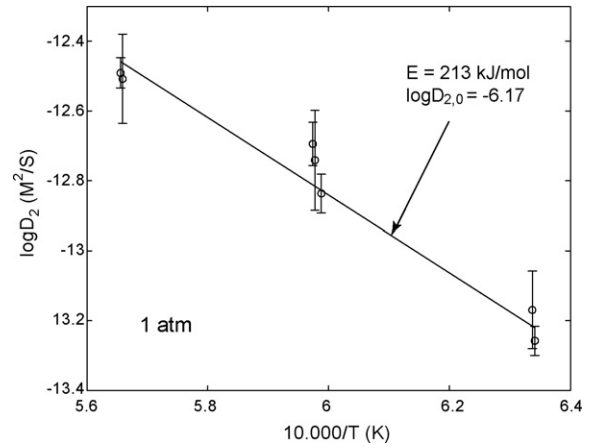


Fig. 5. Arrhenius plot showing Al-vacancy pair diffusion coefficients at 1 atm pressure versus reciprocal temperature.

and magnesium around the defect pair are not very large and mostly cancel (Gourdin and Kingery, 1979a,b).

The variation of the Al^{3+} -vacancy pair diffusion coefficient with temperature and pressure is well described by the Arrhenius equation:

$$D_2 = D_{2,0} \exp \left[\frac{-(E + PV)}{RT} \right] \quad (10)$$

where P is pressure, R is the molar Boltzmann constant, T is temperature (in Kelvins), and E and V are the activation energy and activation volume, respectively. Linear regression of the 1 atm data (Fig. 5) yields an activation energy of 213 ± 32 (2σ) kJ/mol, and a pre-exponential factor $\log_{10} D_{2,0} = -6.17 \pm 0.99$ (m^2/s). The activation energy is somewhat lower than the migration energy of 261 kJ/mol calculated for the Al^{3+} -vacancy pair by Gourdin and Kingery (1979a,b). The activation volume, determined by linear regression of the multi-anvil experimental data at 2273 K and the 1 atm data extrapolated to this temperature (Fig. 6), is 3.22 ± 0.25 (2σ) cm^3/mol , slightly lower than the value of 3.5 ± 0.5 cm^3/mol reported previously (Van Orman et al., 2003) and slightly higher than the activation volume of 3.0 cm^3/mol determined for Mg self-diffusion in that study. To our knowledge, no theoretical estimates are available for the migration volume of trivalent cation-vacancy pairs.

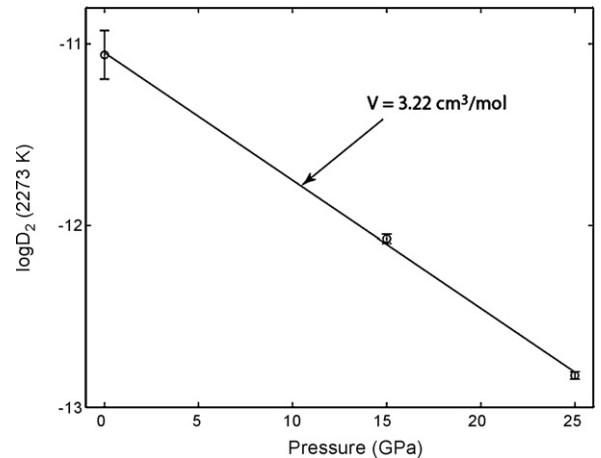


Fig. 6. Al-vacancy pair diffusion coefficients versus pressure, at 2273 K. The point at low pressure represents an extrapolation of the 1 atm experiments, with propagated uncertainty.

6. Discussion

6.1. Al-vacancy site exchange frequency

Diffusion of a bound Al-vacancy pair involves two different types of site exchange: (1) between the vacancy and Al, and (2) between the vacancy and other nearest-neighbor Mg sites. The Mg-vacancy site exchanges reorient the Al-vacancy pair; without them, the Al and vacancy would simply exchange places, back and forth, and no long-range transport would be possible. According to the theory developed by Lidiard (1955), the diffusion coefficient of the impurity-vacancy pair in crystals with the rocksalt structure is related to the two jump frequencies as follows:

$$D_2 = \frac{a^2 \omega_1 \omega_2}{3(\omega_1 + \omega_2)} \quad (11)$$

where a is the distance between Mg and O nearest-neighbors, ω_1 is the frequency of a jump of the vacancy to one of four equivalent Mg positions surrounding the Al, and ω_2 is the frequency of a site exchange between the Al and vacancy. Using Eq. (11) it is possible to solve for ω_2 provided that ω_1 is known. If ω_1 is assumed to be equivalent to the frequency of a site exchange between Mg and vacancy in the absence of a nearby Al^{3+} ion, then its value can be inferred from the vacancy diffusion measurements of Sempolinski and Kingery (1980). Making this assumption, we find that $\omega_2 = 0.419\omega_1$ at 1473 K and $\omega_2 = 0.366\omega_1$ at 1773 K. This implies that in the absence of any binding between Al atoms and vacancies, Al would diffuse somewhat more slowly than Mg.

The motion entropy of Al can be inferred from a similar analysis using the relation $\omega_{2,0} = \nu \exp(S_{\text{Al}}^m/R)$ (e.g., Shewmon, 1989, p. 74, see eqs. 2–28), where $\omega_{2,0}$ is the Al-vacancy site exchange frequency extrapolated to infinite temperature, and ν is the jump attempt frequency, which is approximately equal to the vibrational frequency. The value of $\omega_{2,0}$ is determined from Eq. (11) by extrapolating the vacancy jump frequency to infinite temperature using the Arrhenius relationship determined by Sempolinski and Kingery (1980), and using $D_{2,0}$ determined from the fit of our experimental data to the Arrhenius equation. Assuming that ν for Al is equivalent to the value for Mg used by Sempolinski and Kingery ($1.3 \times 10^{13} \text{ s}^{-1}$), the motion entropy for Al is $12.0 \text{ J mol}^{-1} \text{ K}^{-1}$, one third of the value of $35.8 \text{ J mol}^{-1} \text{ K}^{-1}$ determined for Mg vacancy motion by Sempolinski and Kingery (1980).

6.2. Diffusion of Al and Mg as functions of Al concentration, temperature and pressure

The diffusion coefficient for Al in MgO can be calculated as a function of Al concentration, Al-vacancy pair diffusivity and binding energy using Eq. (7). The Al-vacancy pair diffusivity is given by Eq. (10), with $E = 213 \text{ kJ/mol}$, $V = 3.22 \times 10^{-6} \text{ m}^3/\text{mol}$, and $D_{2,0} = 6.76 \times 10^{-7}$. The self-diffusion coefficient for Mg can be calculated using the equation $D_{\text{Mg}} = x_{\text{V}} D_{\text{V}}$, where D_{V} is the vacancy diffusion coefficient and x_{V} is the fraction of vacant cation sites, excluding those that are bound to Al (the mobility of a vacancy is diminished by a factor of ~30–40 when it is bound to an Al atom, and therefore, bound vacancies would not contribute significantly to Mg transport under most conditions). The vacancy diffusivity can be calculated as a function of temperature and pressure using an Arrhenius equation (e.g., Eq. (10)) with a pre-exponential factor of $3.8 \times 10^{-5} \text{ m}^2/\text{s}$ and activation energy of 220 kJ/mol (Sempolinski and Kingery, 1980) and an activation volume of $3.0 \text{ cm}^3/\text{mol}$ (Van Orman et al., 2003). The cation fraction of unbound vacancies is given by $x_{\text{V}} = x_{\text{Al}}(1/2 - p)$, with p given by Eq. (5).

Fig. 7 shows calculated Al and Mg diffusion coefficients as functions of reciprocal temperature, for three different Al concen-

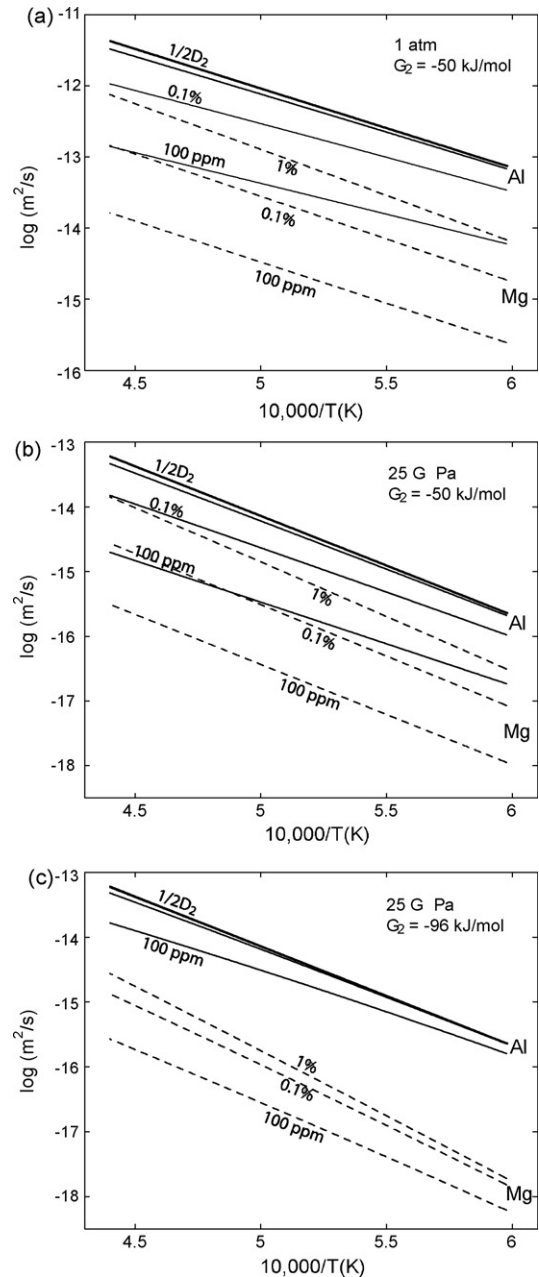


Fig. 7. Calculated diffusion coefficients for Al (solid curves) and Mg (dashed curves) plotted versus reciprocal temperature, at Al concentrations (cation %) of 100 ppm, 0.1 and 1%.

trations (100 ppm, 0.1 and 1%). At atmospheric pressure (Fig. 7a) the binding energy is assumed to have a constant value of -50 kJ/mol , equivalent to the average binding energy determined from the 1 atm experiments. At the same Al concentration and temperature, the Al diffusion coefficient is approximately an order of magnitude larger than the Mg self-diffusion coefficient. The difference increases at lower temperatures and lower Al concentrations. At an Al concentration of 1% (expressed in terms of the percentage of cation sites occupied by Al) the Al diffusion coefficient is near the limiting value, which is equal to half the pair diffusivity. Note that the curves for Al and Mg have quite different slopes, despite the similarity in activation energy for Mg self-diffusion and Al-vacancy pair diffusion (220 and 213 kJ/mol, respectively). The apparent activation energy for Al diffusion is lower than the activation energy for

the Al-vacancy pair, while the apparent activation energy for Mg is higher than the Mg migration energy. At higher temperatures the fraction of vacancies that are bound to Al decreases, thus increasing the Mg diffusivity and decreasing the Al diffusivity. At low Al concentrations the apparent activation energy for Mg is only slightly higher than the migration energy, because at all temperatures most of the vacancies are unbound, while the apparent activation energy for Al (166 kJ/mol) is much lower than the activation energy for the bound pair. On the other hand, at an Al concentration of 1% most of the vacancies are bound to Al. The apparent activation energy for Al increases to 204 kJ/mol, only slightly lower than the activation energy of the Al-vacancy pair, while the apparent activation energy for Mg increases to 248 kJ/mol, much higher than the Mg migration energy.

Two different binding energies are assumed for diffusion at a pressure of 25 GPa: -50 kJ/mol, the average value for the 1 atm experiments (Fig. 7b), and -96 kJ/mol, the value for the 25 GPa experiment (Fig. 7c). At the higher binding energy, there is a larger contrast in Al and Mg diffusion coefficients, and their dependence on Al concentration is diminished, because the proportion of bound Al-vacancy pairs is high even at low Al concentrations. The strong binding increases the apparent activation enthalpy for Mg diffusion to 384 kJ/mol at 1% Al, which is 30% higher than the migration enthalpy (295 kJ/mol) at 25 GPa pressure.

The calculations shown in Fig. 7 may be a useful guide to self-diffusion of Mg in natural periclase that also contains Cr^{3+} and Fe^{3+} . In particular, if the energy of binding to vacancies is similar for these solutes, then they can be considered together in terms of their influence on the concentration of unbound vacancies, and on the diffusion of divalent cations such as Mg that diffuse by a vacancy mechanism.

7. Conclusions

Cation vacancies are strongly attracted to Al in periclase and form bound pairs that have a strong influence on Al diffusion, and on the diffusion of other cations that diffuse by a vacancy mechanism. We have presented a numerical method for extracting the Al-vacancy pair binding energy and diffusion coefficient from Al diffusion profiles in periclase, and have applied it to experiments at 1 atm to 25 GPa and 1577–2273 K. The free energy of binding between an Al^{3+} ion and a cation-vacancy is between -44 and -60 kJ/mol in all but one experiment. No systematic temperature dependence is resolvable. One experiment at 25 GPa has a much larger binding energy, -96 kJ/mol. The diffusion coefficient of the Al-vacancy pair has an Arrhenian dependence on temperature and pressure, with an activation energy $E = 213 \pm 32$ kJ/mol, pre-exponential factor $\log_{10} D_{2,0} = -6.17 \pm 0.99$ (in m^2/s), and activation volume $V = 3.22 \pm 0.25 \text{ cm}^3/\text{mol}$ (all uncertainties are 2σ values determined from linear least-squares regression). The Al diffusion coefficient depends on the Al-vacancy pair diffusion coefficient and the fraction of Al atoms that are bound to vacancies, and thus has a complicated dependence on Al concentration and temperature. At low Al concentrations the temperature dependence of the Al diffusion coefficient is significantly less than that of the Al-vacancy pair. The formation of Al-vacancy pairs hinders the motion of vacancies through periclase, and must, therefore, diminish the diffusivity of cations that diffuse by a vacancy mechanism but are not bound to vacancies themselves. Calculations are presented for the self-diffusion coefficient of Mg as a function of Al concentration, temperature and pressure. Because the proportion of bound Al-vacancy pairs decreases with increasing temperature, the temperature dependence of the Mg self-diffusion coefficient is stronger than implied

by the Mg motion energy, particularly at higher Al concentrations.

Acknowledgments

Yingwei Fei provided generous access to his lab for the multi-anvil experiments, and Chris Hadidiacos kindly provided assistance with the electron microprobe analyses. Fidel Costa and Laurence Coogan provided insightful comments that improved the presentation of the manuscript. Bernard Bourdon, and all of the staff at the ETH-Zürich, provided hospitality and support while part of this manuscript was written. This material is based upon work supported by the National Science Foundation under Grant No. 0337125.

References

- Balluffi, R.M., 1960. On the determination of diffusion coefficients in chemical diffusion. *Acta Metall.* 8, 871–873.
- Bertka, C.M., Fei, Y., 1997. Mineralogy of the Martian interior up to core-mantle boundary pressures. *J. Geophys. Res.* 102, 5251–5264.
- Bina, C.R., 1998. Lower mantle mineralogy and the geophysical perspective. *Rev. Mine.* 37, 205–239.
- Carroll, J.C.G., Corish, J., Henderson, B., Mackrodt, W.C., 1988. Theoretical study of the defect distribution of trivalent cation impurities in MgO. *J. Mater. Sci.* 23, 2824–2836.
- Cherniak, D.J., Zhang, X.Y., Wayne, N.K., Watson, E.B., 2001. Sr, Y, and REE diffusion in fluorite. *Chem. Geol.* 181, 99–111.
- Chick, L.A., Pederson, L.R., Maupin, G.D., Bates, J.L., Thomas, L.E., Exarhos, G.J., 1990. Glycine-nitrate combustion synthesis of oxide ceramic powders. *Mater. Lett.* 10, 6–13.
- Crank, J., 1975. *The Mathematics of Diffusion*, 2nd ed. Clarendon Press, Oxford, 414 pp.
- Gourdin, W.H., Kingery, W.D., 1979a. The defect structure of MgO containing trivalent cation solutes: shell model calculations. *J. Mater. Sci.* 14, 2053–2073.
- Gourdin, W.H., Kingery, W.D., 1979b. The defect structure of MgO containing trivalent cation solutes: the oxidation-reduction behaviour of iron. *J. Mater. Sci.* 14, 2074–2082.
- Hirsch, L.M., Shankland, T.J., 1991. Equilibrium point-defect concentrations in MgO: understanding the mechanisms of conduction and diffusion and the role of Fe impurities. *J. Geophys. Res.* 96, 385–403.
- Holzappel, C., Rubie, D.C., Mackwell, S., Frost, D.J., 2003. Effect of pressure on Fe-Mg interdiffusion in $(\text{Fe}_x\text{Mg}_{1-x})\text{O}$, ferropericlase. *Phys. Earth Planet. Interiors* 139, 21–34.
- Holzappel, C., Rubie, D.C., Frost, D.J., Langenhorst, F., 2005. Fe-Mg interdiffusion in $(\text{Mg,Fe})\text{SiO}_3$ perovskite and lower mantle reequilibration. *Science* 309, 1707–1710.
- Ita, J., Cohen, R.E., 1997. Effects of pressure on diffusion and vacancy formation in MgO from non-empirical free-energy integrations. *Phys. Rev. Lett.* 79, 3198–3201.
- Jacobsen, S.D., Reichmann, H.-J., Spetzler, H.A., Mackwell, S.J., Smyth, J.R., Angel, R.J., McCammon, C.A., 2002. Structure and elasticity of single-crystal $(\text{Mg,Fe})\text{O}$ and a new method of generating shear waves for gigahertz ultrasonic interferometry. *J. Geophys. Res.* 107, Art. No. 2037.
- Keneshea, F.J., Fredericks, W.J., 1963. Diffusion of lead ions in potassium chloride. *J. Chem. Phys.* 38, 1952–1958.
- Kröger, F.A., 1974. *The Chemistry of Imperfect Crystals*, 2nd ed. North-Holland, New York.
- Lidiard, A.B., 1955. Impurity diffusion in crystals (mainly ionic crystals with the sodium chloride structure). *Phil. Mag.* 46, 1218–1237.
- Mackwell, S., Bystricky, M., Sproni, C., 2005. Fe-Mg interdiffusion in $(\text{Mg,Fe})\text{O}$. *Phys. Chem. Mine.* 32, 418–425.
- Perkins, R.A., Rapp, R.A., 1973. The concentration-dependent diffusion of chromium in nickel oxide. *Metall. Trans.* 4, 193–205.
- Sempolinski, D.R., Kingery, W.D., 1980. Ionic conductivity and magnesium vacancy mobility in magnesium oxide. *J. Am. Ceram. Soc.* 63, 664–669.
- Shewmon, P., 1989. *Diffusion in Solids*. Salem, TMS, 246 pp.
- Stachel, T., Harris, J.W., Brey, G.A., Joswig, W., 2000. Kankan diamonds (Guinea) II: lower mantle inclusion parageneses. *Contrib. Mine. Petrol.* 140, 16–27.
- Stretton, I., Heidelberg, F., Mackwell, S., Langenhorst, F., 2001. Dislocation creep of magnesiowüstite ($\text{Mg}_{0.8}\text{Fe}_{0.2}\text{O}$). *Earth Planet. Sci. Lett.* 194, 229–240.
- Takafuji, N., Hirose, K., Mitome, M., Bando, Y., 2005. Solubilities of O and Si in liquid iron in equilibrium with $(\text{Mg,Fe})\text{SiO}_3$ perovskite and the light elements in the core. *Geophys. Res. Lett.* 32, Art. No. L06313.
- Van Orman, J.A., Fei, Y., Hauri, E.H., Wang, J., 2003. Diffusion in MgO at high pressures: constraints on deformation mechanisms and chemical transport at the core-mantle boundary. *Geophys. Res. Lett.* 30, Art. No. 1056.

- van Westrenen, W., Van Orman, J.A., Watson, H., Fei, Y., Watson, E.B., 2003. Assessment of temperature gradients in multi-anvil assemblies using spinel layer growth kinetics. *Geochem. Geophys. Geosyst.* 4, Art. No. 1036.
- Watson, E.B., Price, J.D., 2002. Kinetics of the reaction $\text{MgO} + \text{Al}_2\text{O}_3 \rightarrow \text{MgAl}_2\text{O}_4$ and Al-Mg interdiffusion in spinel at 1200 to 2000 degrees C and 1.0 to 4.0 GPa. *Geochim. Cosmochim. Acta* 66, 2123–2138.
- Wood, B.J., 2000. Phase transformations and partitioning relations in peridotite under lower mantle conditions. *Earth Planet. Sci. Lett.* 174, 341–354.
- Yamazaki, D., Kato, T., Yurimoto, H., Ohtani, E., Toriumi, M., 2000. Silicon self-diffusion in MgSiO_3 perovskite at 25 GPa. *Phys. Earth Planet. Interiors* 119, 299–309.